

## Regional climate model downscaling of the U.S. summer climate and future change

Xin-Zhong Liang,<sup>1</sup> Jianping Pan,<sup>1</sup> Jinhong Zhu,<sup>1</sup> Kenneth E. Kunkel,<sup>1</sup> Julian X. L. Wang,<sup>2</sup> and Aiguo Dai<sup>3</sup>

Received 19 September 2005; revised 7 December 2005; accepted 30 January 2006; published 31 May 2006.

[1] A mesoscale model (MM5)-based regional climate model (CMM5) integration driven by the Parallel Climate Model (PCM), a fully coupled atmosphere-ocean-land-ice general circulation model (GCM), for the present (1986–1995) summer season climate is first compared with observations to study the CMM5's downscaling skill and uncertainty over the United States. The results indicate that the CMM5, with its finer resolution (30 km) and more comprehensive physics, simulates the present U.S. climate more accurately than the driving PCM, especially for precipitation, including summer mean patterns, diurnal cycles, and daily frequency distributions. Hence the CMM5 downscaling provides a credible means to improve GCM climate simulations. A parallel CMM5 integration driven by the PCM future (2041–2050) projection is then analyzed to determine the downscaling impact on regional climate changes. It is shown that the CMM5 generates climate change patterns very different from those predicted by the driving PCM. A key difference is a summer “warming hole” over the central United States in the CMM5 relative to the PCM. This study shows that the CMM5 downscaling can significantly reduce GCM biases in simulating the present climate and that this improvement has important consequences for future projections of regional climate changes. For both the present and future climate simulations, the CMM5 results are sensitive to the cumulus parameterization, with strong regional dependence. The deficiency in representing convection is likely the major reason for the PCM's unrealistic simulation of U.S. precipitation patterns and perhaps also for its large warming in the central United States.

**Citation:** Liang, X.-Z., J. Pan, J. Zhu, K. E. Kunkel, J. X. L. Wang, and A. Dai (2006), Regional climate model downscaling of the U.S. summer climate and future change, *J. Geophys. Res.*, *111*, D10108, doi:10.1029/2005JD006685.

### 1. Introduction

[2] Regional climate model (RCM) integrations are recognized as a valuable dynamic downscaling approach to bridge the gap between general circulation model (GCM) climate simulations and projections at global coarse resolutions and impact assessment applications at local to regional scales [Mearns *et al.*, 1999; Giorgi *et al.*, 2001; Leung *et al.*, 2003]. It is widely recognized that RCMs are more skillful at resolving orographic climate effects than the driving GCMs, especially for near-surface variables. This improvement is a direct result of the spatial resolution enhancement in RCMs versus GCMs [Leung and Qian, 2003]. Certain GCM systematic biases, however, cannot be removed simply by increasing spatial resolution [Risbey and Stone, 1996; Marshall *et al.*, 1997]. A more important

factor is that many recent RCMs incorporate more realistic representation of key physical processes (particularly surface-atmosphere and cloud-radiation interactions) than GCMs [Han and Roads, 2004]. As such, significant RCM downscaling skill has also been achieved over regions with relatively flat terrain, including the central United States [Liang *et al.*, 2004a, 2004b].

[3] Although model performance has continued to improve, current RCMs still contain important climate biases and downscaling uncertainties that are not fully explained. Many of these RCM deficiencies are sensitive to the representation of physical processes, especially cumulus, radiation and surface parameterizations [Vidale *et al.*, 2003; Liang *et al.*, 2004a, 2004b], and in principle the model deficiencies can be substantially reduced or eventually eliminated through better mechanism understanding and resultant model improvement. Before that occurs, confidence in nested climate change projections can only be built upon the credibility of the GCM-driven RCM in simulating the present climate. A more troublesome issue is that such RCM credibility is strongly influenced by substantial uncertainties in global reanalyses [Liang *et al.*, 2001, 2004b] and systematic biases in GCM simulations [Räisänen *et al.*,

<sup>1</sup>Illinois State Water Survey, University of Illinois at Urbana-Champaign, Champaign, Illinois, USA.

<sup>2</sup>Air Resources Laboratory, National Oceanic and Atmospheric Administration, Silver Spring, Maryland, USA.

<sup>3</sup>National Center for Atmospheric Research, Boulder, Colorado, USA.

2004]. These uncertainties are integrated into the RCM domain as continuous lateral forcings during, respectively, the standalone RCM validation and the nested GCM-RCM evaluation experiment. Consequently, present climate simulations and future change projections at local to regional scales can differ greatly among different RCMs [Pan *et al.*, 2001] or different driving GCMs [Räisänen *et al.*, 2004] and between the nested RCM and GCM [Han and Roads, 2004]. It is therefore crucial, and the main objective of this study, to conduct a rigorous evaluation prior to actual impact assessment applications of any nested GCM-RCM system. Here we focus on the physical processes that determine individual GCM and RCM biases as well as differences in both the present climate and future changes between the simulations with and without the RCM downscaling.

[4] RCM model evaluation and climate change studies have often focused on mean state conditions. Studies on model biases and projected changes in the diurnal cycle and frequency distribution are rare. These latter fields are, however, as important as the mean state for practical applications. In particular, the diurnal cycle and frequency distribution of precipitation and surface air temperature, and their future changes, are critical for air quality modeling [National Research Council, 1991]. The precipitation diurnal cycle is by itself a challenging issue in the climate modeling community. For the United States, the main features are the eastward propagation of convective systems and the nocturnal precipitation maxima over the Great Plains during summer, which can be reproduced by very few GCMs and RCMs [Dai *et al.*, 1999a; Zhang, 2003; Davis *et al.*, 2004; Liang *et al.*, 2004a]. This study emphasizes the diurnal cycle and frequency distribution of temperature and precipitation as well as their sensitivity to RCM cumulus parameterization schemes.

## 2. Model Simulations and Observations

[5] The GCM present (1986–1995) and future (2041–2050) climates in this study were simulated by the Parallel Climate Model (PCM) [Washington *et al.*, 2000]. The PCM is a coupled climate system model consisting of an atmospheric GCM, an ocean GCM, a land surface model, and a sea-ice model. The coupling is done through a flux coupler that computes and exchanges interfacial fluxes among the component models. The PCM does not use flux adjustments. It produces a stable climate (except for the deep oceans where there is a small cooling with time) in its control run that is comparable to observations [Washington *et al.*, 2000] and has El Niño amplitude and spatial patterns [Meehl *et al.*, 2001] that are comparable to observed. The forcing in the present (based on observations) and future (using a business-as-usual emissions scenario) climate simulations includes greenhouse gases (CO<sub>2</sub>, CH<sub>4</sub>, N<sub>2</sub>O, O<sub>3</sub>, and CFCs) and sulfate aerosols (see Dai *et al.* [2001a] for details). The effective CO<sub>2</sub> concentrations are approximately 390 and 560 ppmv for the present and future periods, respectively. The PCM simulations are described by Dai *et al.* [2001b, 2004].

[6] The RCM used in this study is a climate extension of the fifth-generation Pennsylvania State University–National Center for Atmospheric Research Mesoscale Model (MM5)

(J. Dudhia *et al.*, PSU/NCAR Mesoscale Modeling System Tutorial Class Notes and User's Guide: MM5 Modeling System Version 3, available online at <http://www.mmm.ucar.edu/mm5/documents/>, 2005), hereafter referred to as CMM5. The model formulation and computational domain (Figure 1) were described by Liang *et al.* [2004b]. It was demonstrated that the CMM5, with a horizontal grid spacing of 30 km, has considerable downscaling skill over the United States, producing more realistic regional details and overall smaller biases than the driving global National Centers for Environmental Prediction–Department of Energy Atmospheric Model Intercomparison Project II reanalysis (R-2) [Kanamitsu *et al.*, 2002]. Improved skill was identified in both the diurnal and annual cycles of precipitation [Liang *et al.*, 2004a, 2004b] as well as in seasonal and interannual variations of soil temperature and moisture [Zhu and Liang, 2005].

[7] The actual CMM5 performance, however, was found to be region dependent and sensitive to the choice of cumulus parameterization schemes, whose skills are highly climate regime selective. The Grell [1993] scheme realistically simulates the nocturnal precipitation maxima over the central United States and the associated eastward propagation of convective systems from the Rockies to the Great Plains where the diurnal timing of convection is controlled by large-scale tropospheric forcing, whereas the Kain and Fritsch [1993] scheme is more accurate for the late afternoon peaks in the southeast where moist convection is governed by near-surface forcing [Liang *et al.*, 2004a]. Summer rainfall amounts in the North American Monsoon region are very poorly simulated by the Grell scheme but well reproduced by the Kain-Fritsch scheme, whereas rainfall amounts from moist convection in the southeast are underestimated by the former and overestimated by the latter [Liang *et al.*, 2004b]. Such drastic contrasts motivate an explicit comparison of the CMM5-simulated climate changes using the two cumulus schemes. The differences provide a measure of uncertainty in RCM downscaling of GCM climate simulations. Hereafter, the PCM-driven CMM5 simulations using the Grell and Kain-Fritsch schemes, with everything else being identical, are referred to as PGR and PKF, respectively.

[8] There are several key differences in physical parameterizations between the PCM and the CMM5. The PCM uses a cumulus parameterization by Zhang and McFarlane [1995] for penetrative convection and Hack [1994] for shallow convection. The PCM employs the land surface model of Bonan [1996] while CMM5 uses the Oregon State University (OSU) model [Chen and Dudhia, 2001]. The cloud-radiation interactions in PCM are described by Kiehl *et al.* [1998] while CMM5 follows Liang *et al.* [2004b].

[9] The PCM data archives include 6-hourly fields for surface pressure, surface air (2-m) temperature, and vertical profiles of temperature, humidity and wind in terrain-following sigma layers on the T42 (~2.8° or approximately 300 km) grid. The fields were first vertically interpolated to constant pressure levels [Trenberth *et al.*, 1993] and then horizontally mapped (bilinear in longitude and latitude directions) onto the 30-km CMM5 grid. The resulting fields were used to construct the initial conditions and time-varying lateral boundary conditions (LBCs) that drive the CMM5. In addition, PCM surface

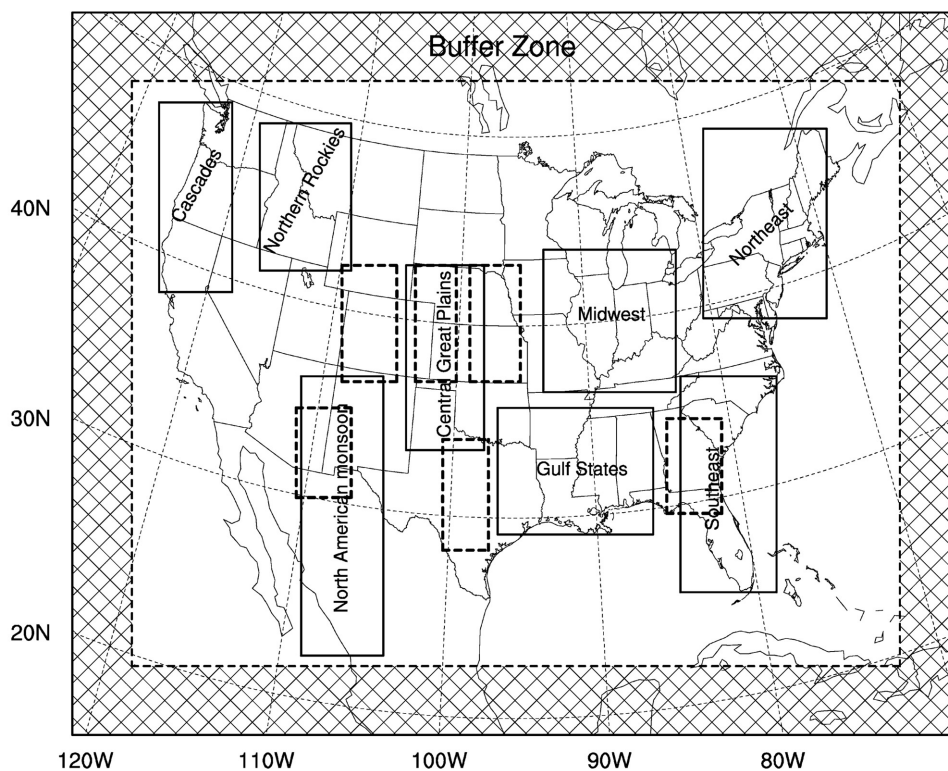


**Figure 1.** CMM5 computational domain. Outlined are eight named regions with solid boxes that characterize the model skills in simulating precipitation annual cycles [Liang *et al.*, 2004b] and six smaller regions with dashed boxes that represent distinct summer rainfall diurnal cycle patterns [Liang *et al.*, 2004a]. The hatched edge areas are the buffer zones, where lateral boundary conditions are specified.

skin temperature outputs were diurnally averaged to produce daily mean sea surface temperature (SST), which was used by the CMM5 as ocean surface boundary conditions [Liang *et al.*, 2004b]. Since the PCM archives contain no data for soil temperature and moisture, these variables in the CMM5 were initialized from the R-2 product.

[10] This study focuses on the summer (June, July, and August) months, when U.S. climate (especially precipitation) modeling strongly depends on the representation of interactions among atmospheric convection, clouds, radiation, and land surface processes [Liang *et al.*, 2004a, 2004b]. As such, the impact of the RCM downscaling is more evident in summer, except for regions dominated by orographic forcing where downscaling produces superior results year-round compared to the driving GCM. Initially, a 6-year continuous PGR integration was conducted starting from 1 April 1990. The resulting 1995 summer mean precipitation and surface air temperature were compared with those from a 5-month run initialized on 1 April 1995. The differences between the two were found to be relatively small compared to interannual variability and uncertainty from a typical computer compiler change, indicating that a 2-month spin-up is sufficient. Therefore, for all CMM5 runs, a segmented integration of every year initiated on 1 April and ending on 31 August was conducted to reduce the computational burden. The 3-hourly model outputs during the last 3 months of each run are used in the subsequent analyses.

[11] Several daily data sets were used for validation during 1986–1995. For the wind circulation at 850 hPa, the R-2 data were taken as the best proxy of observations because they assimilated all available observations. They were available on a global  $2.5^\circ$  longitude by  $2.5^\circ$  latitude grid mesh. Daily precipitation data were a composite of three analysis sources, all based on gauge observations over land. The data source and processing procedures were described by Liang *et al.* [2004b]. The final composite analysis contains daily mean precipitation on the CMM5 grid over the United States and Mexico during the entire validation period. These data do not cover Canada. For surface air temperature, daily mean values were constructed from the average of daily maximum and minimum temperature measurements at 7235 National Weather Service cooperative observer stations over the United States. A constant lapse rate factor based on the individual station altitude was first subtracted from the station observation and the resulting values were then mapped onto the CMM5 grid via the Cressman objective analysis similar to precipitation (see Liang *et al.* [2004b] for details). Finally, the lapse rate factor based on the local CMM5 terrain height was added back to the objectively analyzed values.

[12] For the diurnal cycle validation, hourly precipitation amounts were derived from quality-controlled rain gauge records during 1986–1995 at about 2500 stations on a  $2.5^\circ$  longitude by  $2^\circ$  latitude grid [Higgins *et al.*, 1996],

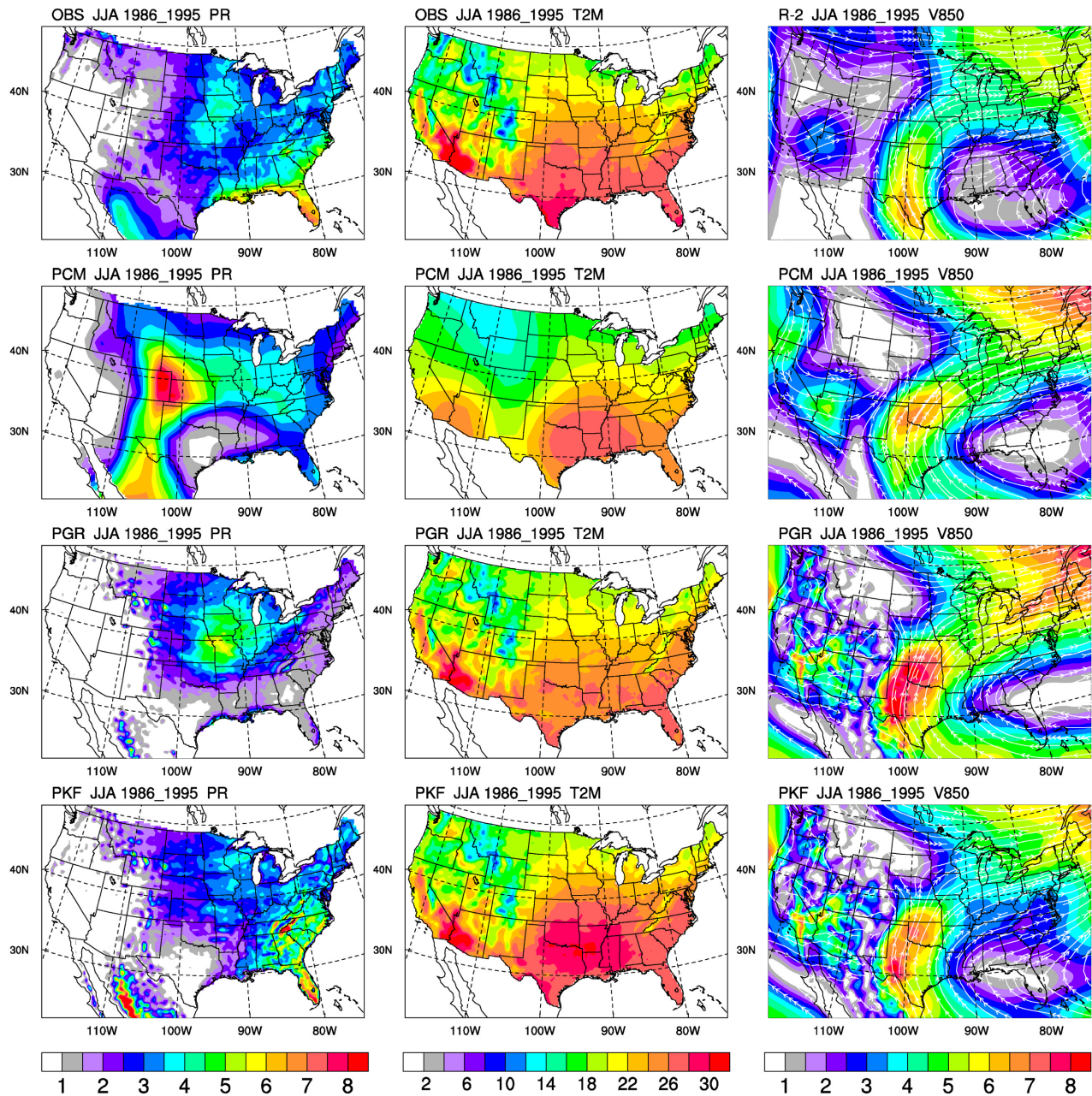


**Figure 2.** Geographic distributions of summer mean (left) precipitation ( $\text{mm d}^{-1}$ ), (middle) surface air temperature ( $^{\circ}\text{C}$ ), and (right) 850-hPa wind ( $\text{m s}^{-1}$ ) averaged during 1986–1995 as observed (OBS), simulated by the PCM, and downscaled by the CMM5 using the Grell (PGR) and Kain-Fritsch (PKF) cumulus scheme. For wind, colors represent the speed while unit vectors denote the direction.

while 3-hourly surface air temperatures were obtained from a climatology (1976–1997) based on synoptic reports at weather stations [Dai and Trenberth, 2004]. Given their coarse resolutions, both hourly precipitation and 3-hourly temperature data and all variables from the R-2 and driving PCM outputs were mapped onto the CMM5 grid using bilinear spatial interpolation. All observational data, except the 3-hourly temperature (1986–1995). These spatial and temporal correspondences facilitate quantitative comparisons among observations, the

driving PCM simulations and the RCM downscaling integrations.

### 3. Present Climate Validation

[13] Figure 2 (left column) compares summer average precipitation during 1986–1995 from the PCM and CMM5 simulations with observations. The PCM simulation is poor, with a rainfall maximum centered in the Great Plains, which is further west and much stronger than the observed center in Iowa. The PGR simulation is more realistic over the

central United States: the intense Great Plains maximum is removed and the maximum over the central United States is in good agreement with observations. The result agrees with *Han and Roads* [2004], who showed the same PCM problem and RCM downscaling improvement and concluded that the difference was not due to the resolution enhancement but rather to the better physics representation in the RCM. In addition, the observed large rainfall over the southeast United States is not captured by either PCM or PGR. A recent study [*Liang et al.*, 2004b] found a marked sensitivity of summer precipitation to the cumulus schemes. When the CMM5 was driven by the R-2, the Grell scheme produced better simulations in the central United States while the Kain-Fritsch scheme was superior in the North American Monsoon region and the southeast United States. Similarly, as compared with the PGR, the PKF produces a much improved pattern in the southeast United States in Figure 2, although it is too dry in the central United States.

[14] The PCM simulation of the summer average 2-m temperature is in general agreement with observations (Figure 2, middle column). The main differences are the smoothed pattern in the west and overall cold biases. Both CMM5 simulations capture the main topographically induced variations in the west and are somewhat warmer than the PCM in the east, in better agreement with observations. The PGR simulation is slightly cooler than observations in the south along the Gulf coast particularly over Texas, while the PKF has a relatively large warm bias. This sensitivity of the 2-m temperature to the cumulus parameterization is quite significant and occurs in conjunction with the precipitation difference discussed above. The Kain-Fritsch scheme tends to produce a vertical heating profile that warms and dries too much near the cloud base. This can ultimately affect surface temperature through turbulent mixing at the top of the planetary boundary layer (PBL; J. Kain, personal communication, 2004). Given various feedbacks, the PKF simulates a weaker low-level flow (see below), which provides more time for local surface heating to accumulate. Also, enhanced convection in the southeast and the associated latent heating may produce an overall warmer atmospheric column over a broad region.

[15] The PCM simulation of the summer mean 850 hPa wind (Figure 2, right column) captures the general observed pattern of strong southerly flow into the central United States around the subtropical ridge. However, the flow is somewhat stronger than the R-2 and exhibits more curvature, not penetrating as deeply into the continental interior. Interestingly, both CMM5 simulations actually produce even stronger southerly flow. The result agrees with *Giorgi et al.* [1998], who found that the RCM downscaling yields a more intense low-level jet (LLJ) than the driving GCM because of finer resolution and better orographic treatment. As compared with the PGR, the PKF generates weaker southerly flow over the central United States, in better agreement with the R-2. These comparisons of flow strength may not indicate actual model biases because the R-2 flow is based on a model assimilation incorporating twice per day observations that are not timed ideally. Specifically, the maximum LLJ speeds occur between 00Z and 12Z in observations; thus there may be a low bias of unknown magnitude in the R-2 maximum [*Liang et al.*, 2001]. In both CMM5 simulations, the curvature of the flow is in better

agreement with the R-2, resulting in deeper penetration into the continental interior. The PCM flow patterns do not explain its strong precipitation maximum in the Great Plains since there is no evidence of enhanced low-level flow convergence. This suggests deficiencies in physical parameterizations, especially the cumulus scheme [*Xie et al.*, 2004; *Collier and Zhang*, 2005], as the likely source of this feature.

[16] Figure 3 compares summer precipitation and temperature diurnal cycles averaged over 6 key regions outlined in Figure 1 for the PCM and CMM5 simulations. These regions are representative of distinct precipitation diurnal cycle patterns over the United States [*Liang et al.*, 2004a]. As discussed in section 2, the data temporal resolution varies from 6-hourly for the PCM to 3-hourly for the CMM5 to hourly (3-hourly) for observed precipitation (temperature). A spline fit is used to produce the hourly values for the PCM and CMM5 simulations as well as observed temperature. The 6-hourly sample times of the PCM are marked in each plot for reference. Following the practice of *Wallace* [1975] and *Dai et al.* [1999a], the rainfall amounts are normalized by a division of the daily mean at individual grids to enhance the compatibility between observations and simulations. The normalization also facilitates easier comparison with previous studies [e.g., *Liang et al.*, 2004a]. The PCM produces a similar precipitation cycle in all of the regions with a daytime maximum and nighttime minimum, failing to reproduce the observed nighttime peak in the Plains and the flat distribution in the LLJ region. In addition, the PCM maxima are several hours earlier than observed in the three regions with a daytime peak (central Rockies, North American Monsoon, southeast United States). The CMM5 simulations are sensitive to the cumulus scheme. The PGR produces excellent results for the central Rockies, central High Plains, central Plains, and LLJ regions. For the North American Monsoon and southeast U.S. regions, the PKF produces a peak somewhat later than the PGR, in better agreement with observations. As found by *Liang et al.* [2004a], the Kain-Fritsch scheme produces a late afternoon peak in all regions because of its strong sensitivity to local near-surface heating. These results of the CMM5 driven by the PCM are very close to those driven by the R-2 [*Liang et al.*, 2004a], suggesting that the U.S. precipitation diurnal cycle patterns may likely be determined by regional processes and the PCM large-scale circulation is sufficient for reasonable CMM5 downscaling of such patterns.

[17] For temperature, all models reproduce the observed diurnal phase reasonably well because of the dominant effect of solar radiation. One exception is that all simulations tend to have a 3-hour phase lead to observations in the central Rockies and North American Monsoon region. The amplitude or diurnal temperature range (DTR) has important model biases. The PCM-simulated DTR is smaller than observed in the central High Plains and central Plains, larger in the North American Monsoon region, while realistic in the other 3 regions. Both CMM5 simulations produce colder nighttime temperatures and thus larger DTR than observed in the central Rockies, North American Monsoon, LLJ, and southeast United States. For the central High Plains and central Plains, the PKF has larger DTR than observations while the PGR is realistic. There is no obvious link between

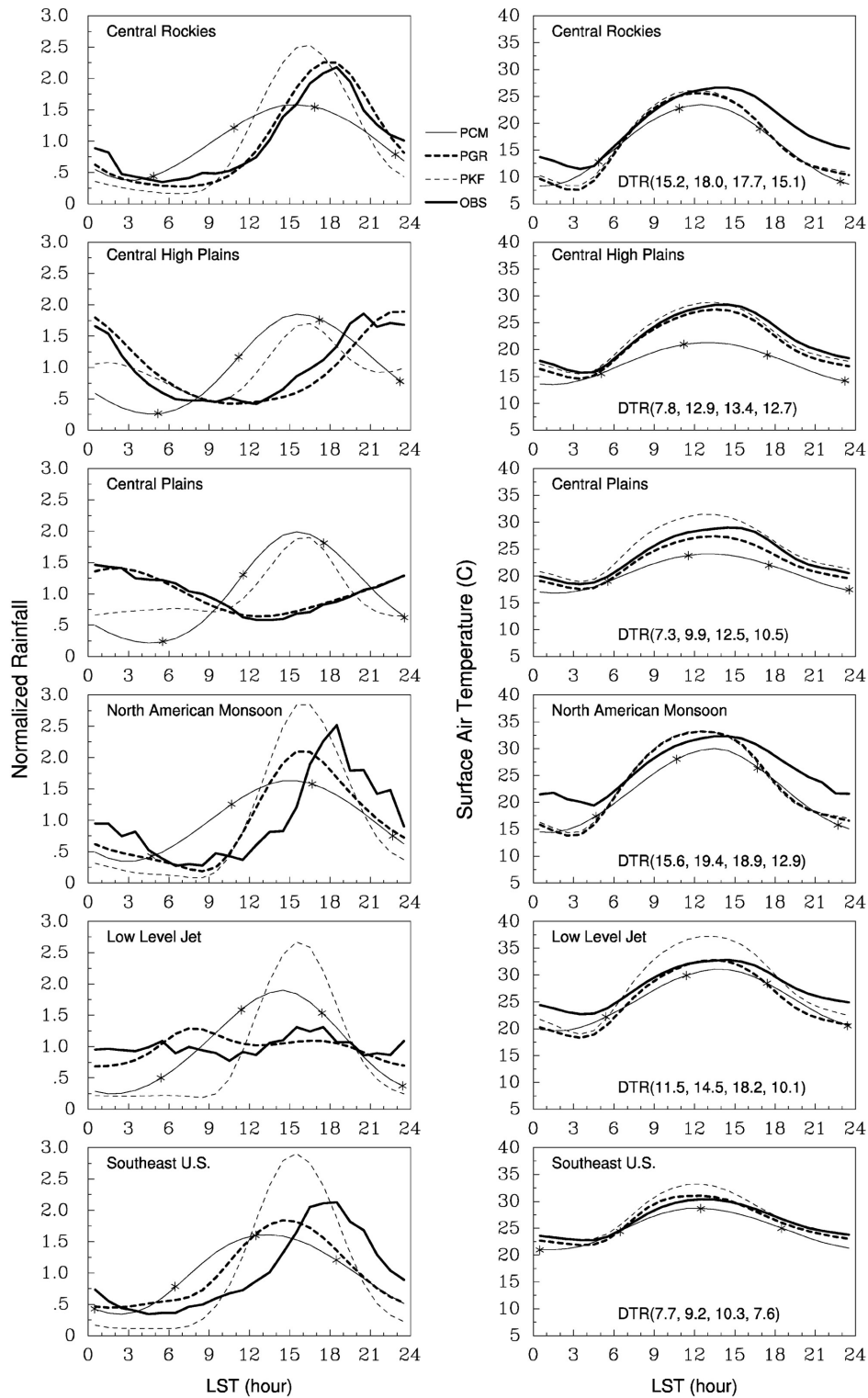


**Figure 3.** The 1986–1995 summer mean diurnal evolutions (relative to LST) of the (left) normalized rainfall and (right) surface air temperature (°C) averaged over six distinct regions: the central Rockies, central high Plains, central Plains, North American Monsoon, low-level jet, and southeast United States (corresponding to the dashed boxes in Figure 1 from west to east columns and north to south rows), as observed (OBS), simulated by the PCM, and downscaled by the CMM5 using the Grell (PGR) and Kain-Fritsch (PKF) cumulus schemes. The stars mark the mean universal times (0000, 0600, 1200, and 1800 UT) when the PCM results are available. The legend for curves is marked in the top middle between the two panels. The diurnal temperature ranges are given in the parentheses following DTR in the order of PCM, PGR, PKF, and OBS.

model biases in temperature and precipitation diurnal cycles. *Dai et al.* [1999b] have shown that low- and middle-level clouds have a dominant damping effect on DTR by reflecting sunlight (and thus reducing the maximum temperature), whereas soil moisture and precipitation have only secondary damping effects (through evaporation).

[18] Figure 4 compares the frequency distributions of summer daily mean rainfall and 2-m air temperature for the eight broad regions outlined in Figure 1 for the PCM and CMM5 simulations. Also shown in the parentheses following the legend are the frequencies, averaged for all grid points in the regions, for the occurrences of dry (<0.25 mm) and heavy rainfall (>15 mm) days. The statistics are based on daily mean values at all CMM5 grid points (there is no spatial averaging) within each region during the entire 30 months. These regions are representative of the dependency on surface characteristics and climate regimes of model skill in simulating precipitation annual cycles [*Liang et al.*, 2004b]. For rainfall, the PCM distributions exhibit substantial differences from observations, except for the Cascades region where summer is the local dry season. The PCM frequencies are too high in the intermediate range (3–15 mm) over the central Great Plains and North American Monsoon regions, while too high at low amounts in the remaining regions. Except for the Cascades region, the PCM frequencies of dry and heavy rainfall days are generally too low, especially for dry days. The CMM5 distributions are generally in better agreement with observations, but the frequencies for dry days are overestimated. For the Cascades, northern Rockies, central Great Plains, Midwest, and northeast regions, the agreement with observations is good for both cumulus schemes, including heavy rainfall days. In the southeast, Gulf states, and North American Monsoon regions, the PKF produces more frequent intermediate rainfall days than the PGR, generally in better agreement with observations. Both CMM5 simulations generate too few heavy rainfall days in the Gulf states region while the agreement in the southeast region is much better for the PKF than the PGR. For temperature, the PCM exhibits cold mean biases over most of the regions, especially in the central Great Plains, southeast, and North American Monsoon regions. Compared with observations, the PCM distribution is shifted systematically to colder temperatures in the southeast and Midwest, is broader in the Gulf states, and is skewed with a shorter tail at high temperatures in other regions. Over the northern Rockies, central Great Plains, southeast, and North American Monsoon regions, the CMM5 with either cumulus scheme produces distributions closer to observations than the PCM. In contrast, both CMM5 simulations produce distributions shifted to warmer temperatures in the Cascades region. On the other hand, in the Midwest and Gulf states regions, the PKF results in too many very warm days, while the PGR simulates more cool days than observed.

[19] It is not clear what exact mechanisms cause the differences between CMM5 and PCM in simulating the frequency distributions and extreme events of precipitation and temperature. Given the existence of large contrast between the PGR and PKF, we speculate that changes in both resolution and physics representation (especially cumulus parameterization) may play an important role for these differences.

#### 4. Future Climate Change Projection

[20] Figure 5 (left column) compares summer mean precipitation changes ( $\text{mm d}^{-1}$ ) from 1986–1995 to 2041–2050 as projected by the PCM and downscaled by the CMM5. The PCM simulation shows increases (greater than  $0.5 \text{ mm d}^{-1}$ ) in the southeast United States and decreases (less than  $-0.5 \text{ mm d}^{-1}$ ) along the Texas-Mexico border. The CMM5 produces less spatially coherent changes, which are of smaller magnitude and of mixed sign. In particular, the southeast rainfall increase in the PCM is absent in the PGR and weak in the PKF. Both CMM5 simulations show scattered areas of rainfall decreases with magnitude greater than  $0.2 \text{ mm d}^{-1}$  along the Texas-Mexico border. They also project slightly wetter (drier) conditions in much of the central United States (central-northern Rockies) than the PCM. However, statistical significance thresholds (estimated at an absolute value of  $1\text{--}2 \text{ mm d}^{-1}$  or greater) are generally higher than these differences. Indeed, the high spatial incoherence (noisiness) of the pattern suggests that most differences may not be physically significant or otherwise should exhibit spatial coherence over scales reflecting the major circulation patterns driving the precipitation climatology.

[21] Comparisons of the PCM versus CMM5 summer mean 2-m temperature changes (Figure 5, middle column) show that the downscaling produces substantially different results. The PCM projects temperature increases in the range of  $1$  to  $3^\circ\text{C}$  over most of the United States, with the largest warming centered in the Midwest and Nevada, but both CMM5 simulations yield warming generally less than  $1^\circ\text{C}$  in the eastern United States. Interestingly, *Pan et al.* [2004] found that the second-generation Regional Climate Model (RegCM2) downscaling produces a local minimum in summer warming over the central United States as compared with the driving Hadley Centre GCM version 2 (HadCM2) projection for 2040–2049 (assuming a 1% annual increase of an effective  $\text{CO}_2$  concentration from 1990). They referred to this effect as a “warming hole” and attributed it to regional land surface feedbacks. This issue will be discussed below.

[22] The PCM and CMM5 projected changes in summer mean 850 hPa wind (Figure 5, right column) are qualitatively similar. All three simulations produce relative anti-cyclonic (cyclonic) circulation changes centered near the Great Lakes (Florida), and off the west coast of Mexico (southwest Canada, not shown). There is no obvious flow difference that can explain the aforementioned contrast in the precipitation and temperature changes over the central United States between the PCM and CMM5 simulations. Over the extreme southeastern United States, an enhanced mean low-level onshore fetch from the weakening subtropical Atlantic high may explain more precipitation increase in the PCM and PKF than PGR. On the other hand, the flow over southern Louisiana becomes less offshore in the PGR, causing larger precipitation increase than the PCM and PKF.

[23] The differences between the future changes projected by the PCM and CMM5 (Figure 6) are sizable in broad areas. For precipitation (left column), the PGR projects relatively wetter conditions in much of the central United States with relatively drier conditions in the southeast and Rocky Mountains, compared to the PCM. The differences

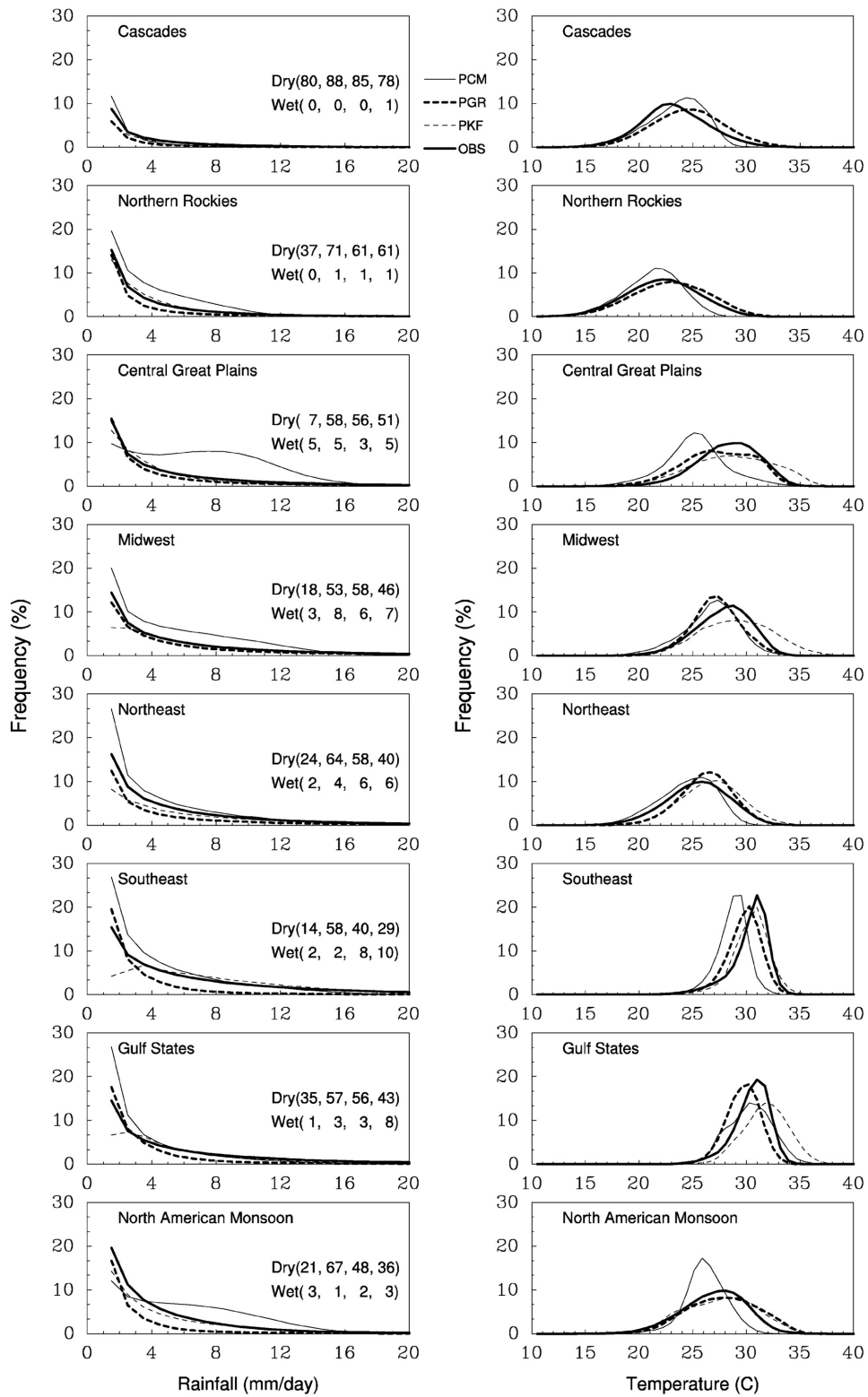
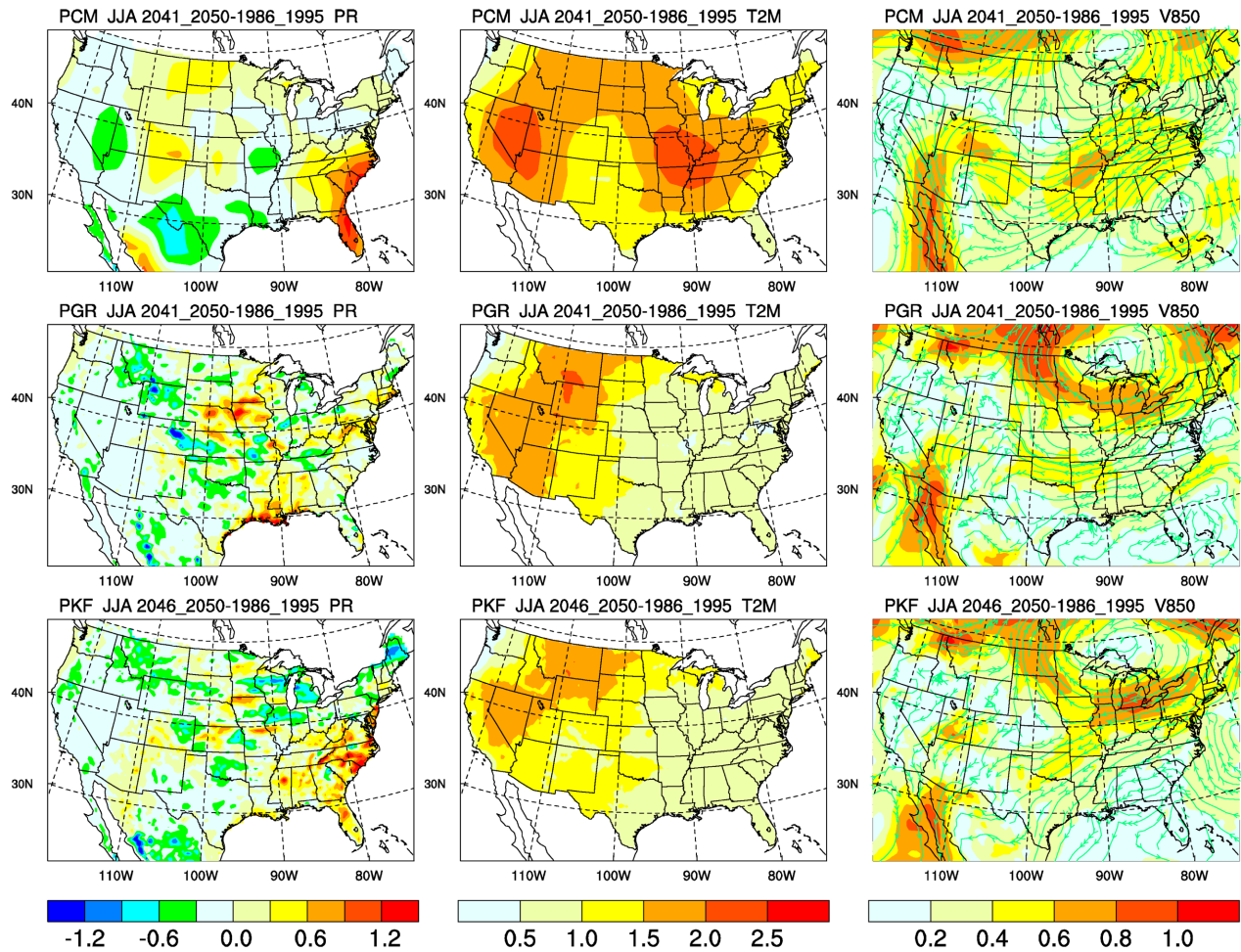


Figure 4



**Figure 5.** Same as Figure 2 except for the projected future changes: differences between the averages during 2041–2050 and 1986–1995.

between the PKF and PCM are generally similar in sign but of somewhat smaller magnitude. For temperature (middle column), the differences from the PCM are similar for PGR and PKF with the most notable feature being relatively cooler conditions simulated by CMM5 in the central United States. This appears to resemble that found by *Pan et al.* [2004], where the warming hole is centered at roughly (38°N, 95°W), while in the present study it is located slightly further to the east (~92°W). Both CMM5 simulations also produce weaker warming over the southwest United States, with the center near Nevada about 1°C less than the PCM. Over the Gulf states, the 850 hPa circulation differences (right column) indicate somewhat greater southerly or southwesterly flow in both CMM5 simulations. This

suggests the possibility of greater moisture advection, a result that is consistent with the relatively higher precipitation along the lower Mississippi River than the PCM.

[24] Changes in summer precipitation and temperature diurnal cycles (Figure 7) are generally small in all three simulations with a few exceptions. The amplitude of the temperature diurnal cycle or DTR in the PCM increases over the central Rockies, whereas all other changes for both temperature and precipitation are small. On the other hand, DTR in the PGR increases over the central Rockies and North American Monsoon regions, where there is also enhanced late afternoon precipitation perhaps associated with the higher midday temperatures. The PGR also generates enhanced

**Figure 4.** The 1986–1995 summer mean frequency (percent) distribution of (left) daily rainfall (mm d<sup>-1</sup>) and (right) surface air temperature (°C) over eight representative regions (from the top down): Cascades, northern Rockies, Central Great Plains, Midwest, northeast, southeast, Gulf states, and North American Monsoon, as observed (OBS), simulated by the PCM, and downscaled by the CMM5 using the Grell (PGR) and Kain-Fritsch (PKF) cumulus schemes. The frequency is defined in bins of a unit interval. The legend for curves is marked in the top middle between the two panels. The numbers in the parentheses following “Dry” and “Wet” show the frequency for dry (<0.25 mm d<sup>-1</sup>) and heavy rainfall (>15 mm d<sup>-1</sup>) days, respectively, in the order of PCM, PGR, PKF, and OBS. All calculations are based on total samples of 10 (years) × 92 (days) × 609–1100 (grids) in each region without temporal or spatial averaging.

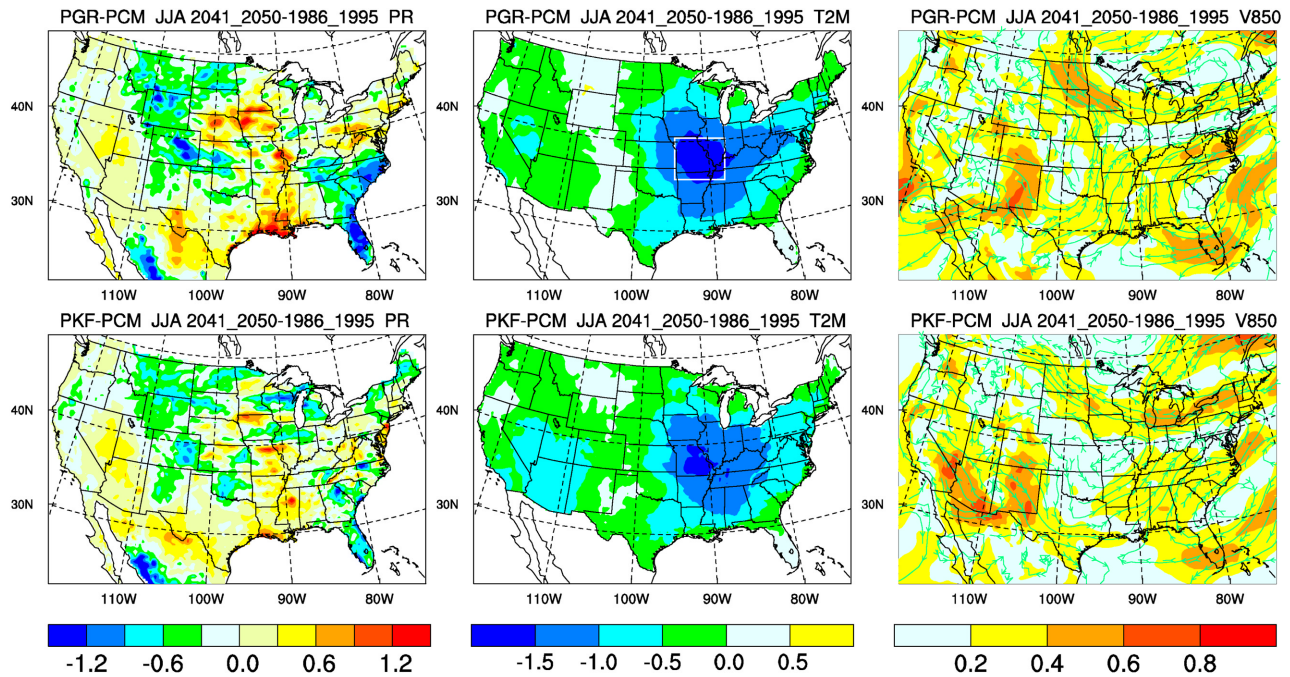


**Figure 6.** Differences in the projected future changes of summer mean (left) precipitation ( $\text{mm d}^{-1}$ ), (middle) surface air temperature ( $^{\circ}\text{C}$ ), and (right) 850-hPa wind ( $\text{m s}^{-1}$ ) as downscaled by the CMM5 using the Grell (PGR) and Kain-Fritsch (PKF) cumulus schemes from those simulated by the PCM. The white box in the PGR temperature plot represents the warming hole core region outlining approximately the area with less than  $-1.5^{\circ}\text{C}$  differences.

(reduced) rainfall in early morning (evening) over both the central Plains and LLJ regions, where little change occurs in the temperature cycle. The only noticeable changes by the PKF are seen with precipitation over the central Rockies and central Plains similar to those in the PGR discussed above. Since the DTR is primarily controlled by clouds, precipitation and soil moisture [Dai *et al.*, 1999b], all of which are still a challenge for climate models to simulate realistically on regional scales. The above DTR changes are likely model dependent.

[25] Changes in summer daily rainfall frequency distributions (Figure 8, left column) are generally small in all three simulations with a few exceptions. For the southeast and, to a lesser extent, the northern Rockies, there is a sizable shift from small to intermediate range days in the PCM, a change not seen at all in the PGR and PKF. Changes in the frequency of dry and heavy precipitation days are quite variable regionally and among models. All models show increases in the frequency of dry days for the Cascades, northern Rockies, Central Great Plains, and North American Monsoon and decreases for the southeast. For the Midwest and northeast, the PCM and PKF simulate increases while the PGR shows a decrease or no change. For the Gulf states, the PCM shows an increase while the PGR and PKF show decreases. For heavy precipitation frequencies, the PCM shows no change or increases in all regions. By contrast, the PGR and PKF both exhibit decreases for the northern Rockies, Central Great Plains, and Midwest; the PGR (PKF) shows a decrease for the North American Monsoon (northeast). For wetter climatic regions, the changes in heavy precipitation frequencies are

mostly a small ( $<10\%$ ) fraction of the current climate values (shown in Figure 4), while for the drier climate regions they are often a much larger fraction (tens of percent). There are few past studies of changes in RCM-simulated precipitation distributions. The Third Assessment Report of the Intergovernmental Panel on Climate Change indicated that RCM simulations of future changes in heavy precipitation events were positive and large, but smaller than indicated by the driving CGCM. Durman *et al.* [2001] found that an RCM downscaling provided a better simulation of heavy precipitation events than the driving GCM for Europe. Kunkel *et al.* [2002] identified regional variations in the ability of an RCM to simulate heavy precipitation events over the United States. The present results are consistent in that the RCM provides a better simulation of extremes and exhibits smaller changes than the PCM, with some regional variations in those findings, as noted above.

[26] The primary feature in the changes in summer daily temperature distributions (Figure 8, right column) is a couplet of decreased frequencies at cooler temperatures and increased frequencies at warmer temperatures, reflecting a shift toward warmer temperatures, the magnitude of that shift varying among models (Figure 5). However, the shapes of the distributions change very little.

[27] Pan *et al.* [2004] suggested that the warming hole results from increased LLJ frequency replenishing seasonally depleted soil moisture, which increases (decreases) evapotranspiration (sensible heating). This causal linkage was investigated here. A wind direction/speed frequency analysis performed for the LLJ and warming hole core regions (Figure 9, top two panels) indicates similar distri-

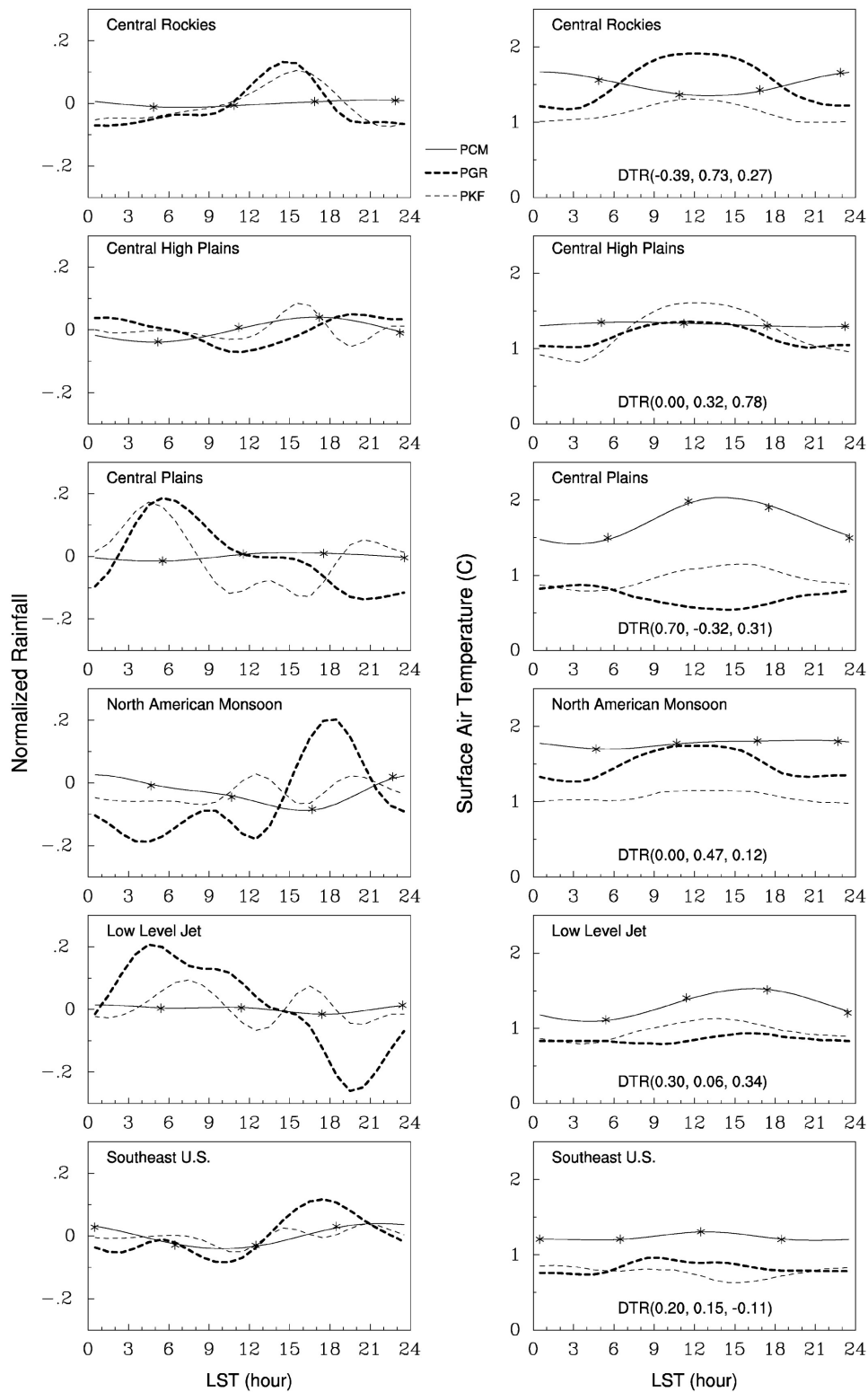


**Figure 7.** Same as Figure 3 except for the projected future changes: differences between the averages during 2041–2050 and 1986–1995.

butions for the PCM and PGR with predominantly southwesterly flow in the LLJ region and southerly flow in the warming hole core region. The projected future changes (Figure 9, bottom two panels) show subtle differences. For

the PCM in the LLJ region, there are decreases of 4% or more in moderate to strong southwesterly flow and increases of 2% in northeasterly flow; these changes would likely result in decreased moisture advection into the central

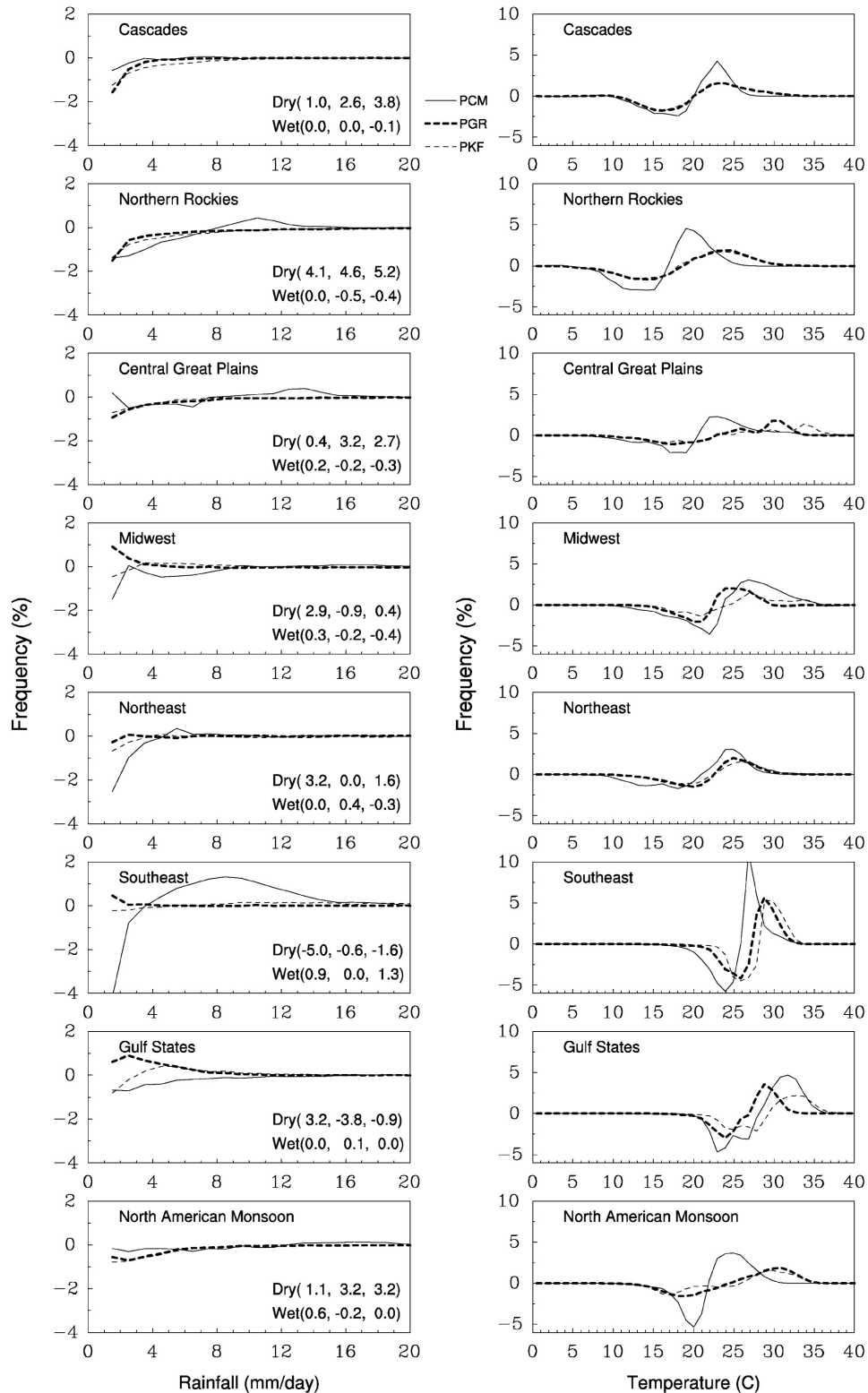


**Figure 8.** Same as Figure 4 except for the projected future changes: differences between the averages during 2041–2050 and 1986–1995.

United States. For the CMM5, the changes are smaller, the major one being a slight shift in flow direction toward a more southerly direction. In the warming hole core region, the changes are similar for both PCM and CMM5 simu-

lations, where the major change is a shift toward stronger southerly wind speeds.

[28] Table 1 compares the projected summer changes in 2-m temperature, precipitation, soil moisture (in the top 1-m

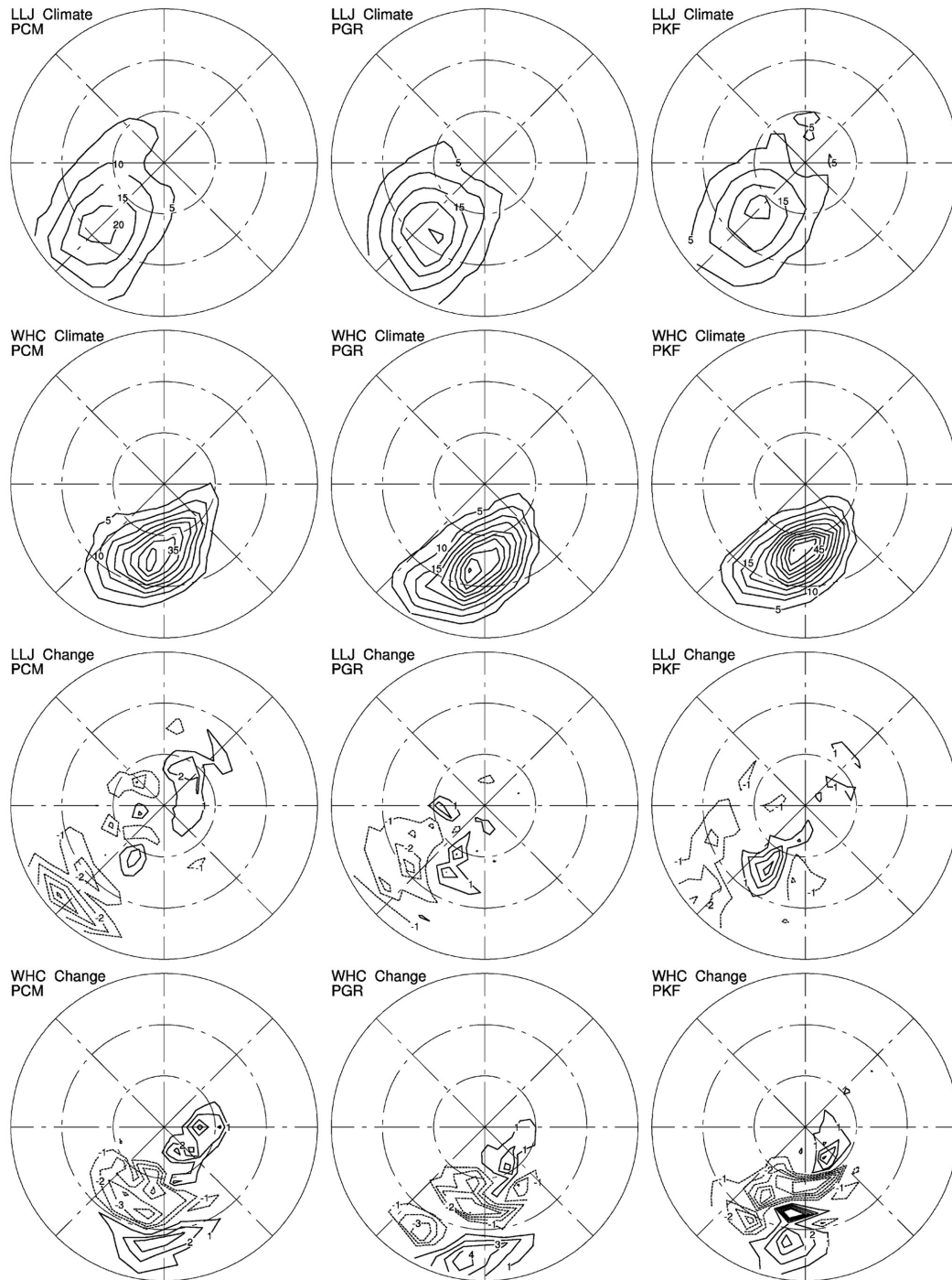


**Figure 9.** Summer 850 hPa wind frequency (percent) distributions projected on a polar coordinate mesh where the speed and direction are represented by radii (5, 10, and 15  $\text{ms}^{-1}$  from the center) and angles (at a  $45^\circ$  interval from north) respectively, as simulated by the (left) PCM, (middle) PGR, and (right) PKF. For a given wind speed and direction, all corresponding wind vectors at each grid within the low-level jet (LLJ, see the dashed box over Texas in Figure 1) or warming hole core (WHC, see the white box in Figure 6) region during the entire period are counted to give the final statistics. The top two panels are for the 1986–1995 climate, and the bottom two panels are for the projected future change (2041–2050 minus 1986–1995). The contour interval is 5% for the present climate and 1% for the future change, and negative values are dashed.

**Table 1.** Projected Summer Changes (2041–2050 Minus 1986–1995) in 2-m Temperature, Precipitation, Soil Moisture in the Top 1-m Layer, Total Cloud Amount, Incident Solar Radiation, Net Solar Radiation, Net Longwave Radiation, Sensible Heat, Latent Heat, Net Radiation, and Total Surface Energy Flux Averaged Over the Warming Hole Core Region as Simulated by the PCM, PGR, and PKF as Well as Their Differences<sup>a</sup>

Variable	Units	PCM	PGR	PKF	PGR – PCM	PKF – PCM	PKF – PGR
T2M	°C	2.18	0.58	0.76	–1.6	–1.42	0.18
PR	mm d <sup>–1</sup>	–0.20	–0.04	0.02	0.16	0.22	0.06
SM	mm	–	8.0	–16.0	–	–	–24.0
CLD	percent	–	0.7	–2.1	–	–	–2.8
SWd	W m <sup>–2</sup>	–	–7.0	4.0	–	–	11.0
SW	W m <sup>–2</sup>	–	–3.5	3.2	–	–	6.7
LW	W m <sup>–2</sup>	–	3.2	0.2	–	–	–3.0
SH	W m <sup>–2</sup>	–17.4	1.1	–0.9	18.5	16.5	–2.0
LH	W m <sup>–2</sup>	6.1	–0.2	–2.5	–6.3	–8.6	–2.3
RAD	W m <sup>–2</sup>	15.0	–0.3	3.4	–15.3	–11.6	3.7
NET	W m <sup>–2</sup>	3.7	0.6	0.0	–3.1	–3.7	–0.6

<sup>a</sup>PCM, Parallel Climate Model; PGR and PKF, PCM-driven CMM5 simulations using the Grell and Kain-Fritsch schemes, respectively. T2M, 2-m temperature; PR, precipitation; SM, soil moisture in the top 1-m layer; CLD, total cloud amount; SWd, incident solar radiation; SW, net solar radiation; LW, net longwave radiation; SH, sensible heat; LH, latent heat; RAD, net radiation; NET, total surface energy flux. See the white box in Figure 6 for warming hole core region. Fluxes are positive toward the surface. Dashes indicate missing data.

layer), total cloud amount, and surface energy budget components averaged over the warming hole core region (see the box in Figure 6) between the PCM and CMM5 simulations. The PCM data archive does not include soil moisture, total cloud amount, and shortwave and longwave radiation components, which necessitates inferences about changes in these variables. The precipitation change, a relatively larger decrease ( $-0.2 \text{ mm d}^{-1}$ ) in the PCM than in the CMM5 (close to zero), is consistent with the low-level flow change discussed above (decreased southwesterly flow in the LLJ region for the PCM). The total cloud amount increases slightly in the PGR and decreases in the PKF. Consequently, the incident radiation decreases in the PGR and increases in the PKF, although not in exact proportion to the cloud amount change (suggesting other effects also contribute). The net radiation change is close to zero in the PGR and small ( $3 \text{ W m}^{-2}$ ) in the PKF relative to the PCM ( $15 \text{ W m}^{-2}$ ). The slightly larger warming in the PKF relative to the PGR is consistent with the small differences in net radiation and sensible heat flux between the two. The CMM5 soil moisture response, although relatively small compared to interannual variations [Changnon *et al.*, 2004], is also consistent with the radiation and latent heat changes. The large radiation increase in the PCM implies sizable cloud reduction. The extra radiation input is compensated in the PCM by a greater sensible heat loss ( $-17 \text{ W m}^{-2}$ ) and relatively smaller latent heat gain ( $6 \text{ W m}^{-2}$ ), with a net balance of about  $4 \text{ W m}^{-2}$ . In both CMM5 simulations, responses in all surface energy components are small and the net balance is close to zero. Thus the hypothesis put forward by Pan *et al.* [2004] in which stronger low-level flow produces greater precipitation and wetter soils and consequently enhanced evapotranspiration and reduced sensible heating does not seem to explain the difference between the CMM5 and PCM projected temperature changes since the CMM5 changes are small. However, the changes in the PCM, opposite in direction to the above hypothesis, are substantial and a possible cause is presented below.

[29] Figure 10 depicts a vertical-zonal cross section of PCM projected changes of temperature and specific humidity extending across the two maxima in warming and the mini-

um in warming in the Great Plains (compare Figure 5). The cross sections provide a two-dimensional perspective on the surface information in Table 1. Note that the surface is much higher than 1000 hPa in the western portions of the domain and the plotted values in the lower portion of the cross sections represent extrapolations, not real features. In the PCM, the warming in the two centers is a maximum at the surface and near, or a short distance to the east (downwind) of, maximum decreases in precipitation. They are also approximately coincident with decreases or a minimum in increases of specific humidity. This suggests that increased radiation (decreased cloud cover) is a major direct cause of these warming centers. By contrast, the warming in the CMM5 simulations is nearly constant with height, not exhibiting a near-surface maximum, and changes in specific humidity are more uniform horizontally. The contrasting vertical structures between the CMM5 and PCM simulations are consistent with the major differences in Table 1. Although it is difficult to separate cause and effect, a primary cause of the PCM warming center in the central United States (Figure 5, coincident with the CMM5 warming hole core in Figure 6) may be a deficient cumulus parameterization scheme. Such deficiencies are the likely cause of the unrealistically strong convection and excessive precipitation over the Great Plains in the PCM present climate simulation (Figure 2). The convection there is further enhanced and extended to the west over the central Rockies in the future climate projection as evident from the precipitation change (Figure 5). The intense convectively driven upward motion over the Great Plains and central Rockies must be balanced in mass by stronger subsidence likely in the downstream region, i.e., the central United States, where precipitation and cloud cover would be reduced and temperature increased via adiabatic warming (plus PBL mixing) or radiative heating. These changes are consistent with the result shown in Table 1. The horizontal circulation fields (bottom two rows of Figure 10) also support this hypothesis: the PCM circulation exhibits enhanced southeast flow on the lee side of the Rockies consistent with stronger low-level convergence in that region, a feature not present in the CMM5 simulations. The PCM warming center in the central United States might disappear if a more realistic cumulus scheme that reduces or

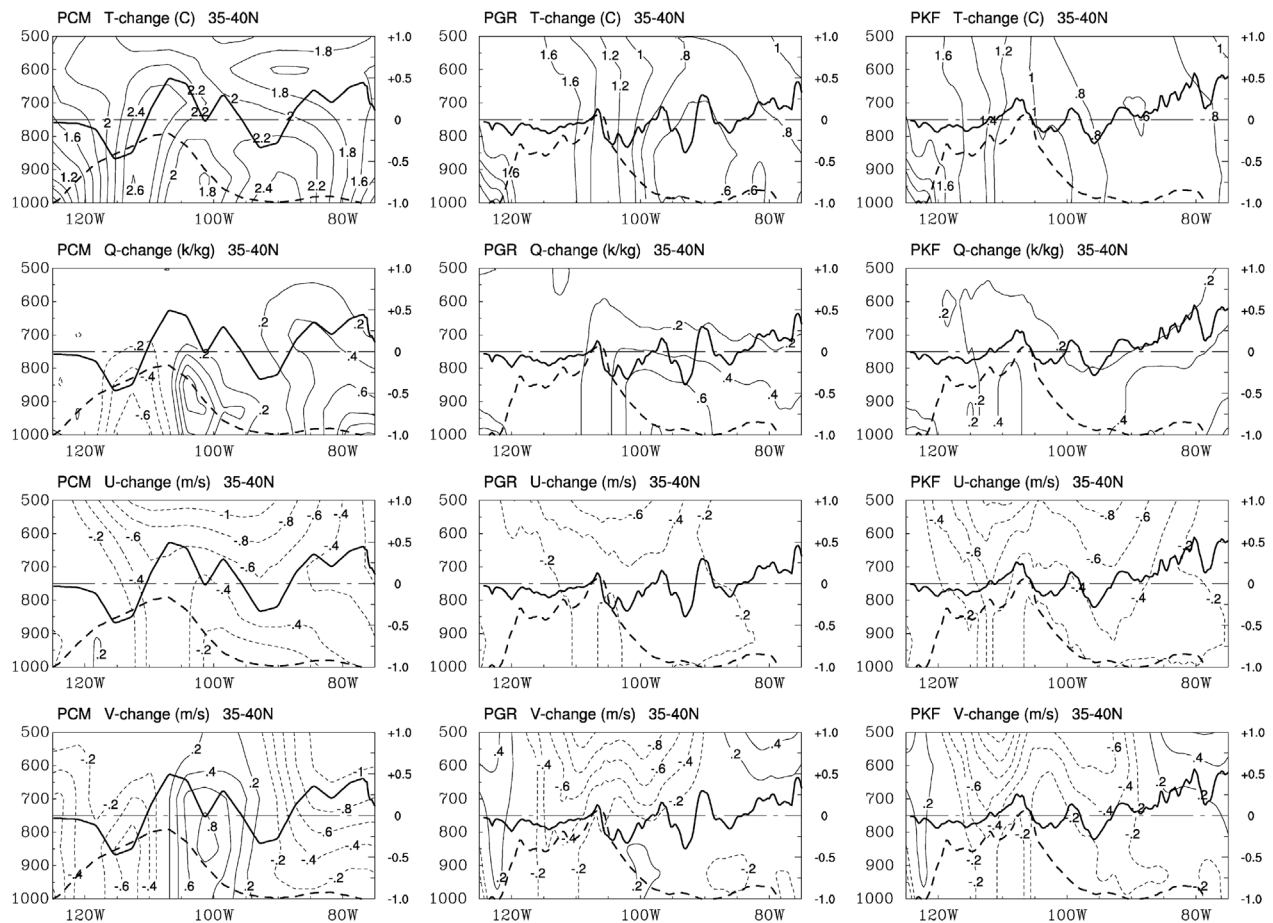


**Figure 10.** Summer longitude-pressure distributions of projected future changes (2041–2050 minus 1986–1995) of vertical profiles for, from top downward, temperature ( $T$ ,  $^{\circ}\text{C}$ ), humidity ( $Q$ ,  $\text{k kg}^{-1}$ ), and zonal ( $U$ ) and meridional ( $V$ ) wind ( $\text{m s}^{-1}$ ) averaged over the belt ( $35^{\circ}$ – $40^{\circ}\text{N}$ ) across the warming hole core as simulated by the (left) PCM, (middle) PGR, and (right) PKF. The scale for pressures (hPa) is on the left, and longitude ( $^{\circ}\text{W}$ ) is on the bottom. Shown also are the corresponding precipitation changes ( $\text{mm d}^{-1}$ , thick solid curve), with the scale on the right. The surface elevation, below which the profiles are extrapolated, is depicted in terms of pressure (hPa, thick dashed curve) using a conversion based on the summer midlatitude standard atmosphere. The contour interval is 0.2 units, and negative values are dashed.

eliminates the convective precipitation bias over the Great Plains is used. Then, the PCM could probably also simulate the much reduced warming over the central United States, lessening the difference with the CMM5. Such improved cumulus schemes are currently available in the new NCAR models [Xie *et al.*, 2004; Collier and Zhang, 2005], providing future opportunities to test our hypothesis.

## 5. Summary and Discussion

[30] The present (1986–1995) and future (2041–2050) climates downscaled by the CMM5 are compared with the driving PCM simulations to study the utility of the regional modeling for skill enhancement important to impact applications in the United States. The present climate simulations are first evaluated against observations to establish model credibility. The results indicate that the CMM5, with its finer resolution and more comprehensive physics, simulates

the present near-surface climate more accurately than the driving PCM, especially for precipitation, including summer means, diurnal cycles and daily frequency distributions. For most of these aspects, the CMM5 results driven by the PCM are close to those driven by the R-2 [Liang *et al.*, 2004a, 2004b], suggesting that the PCM simulated planetary circulation provides reasonable LBCs for the CMM5 to capture the principal characteristics of the observed U.S. climate.

[31] The future climate projections are then compared to determine the downscaling impact on simulations of regional climate changes. Under the business-as-usual emissions scenario, the PCM simulates summer rainfall increases (greater than  $0.5 \text{ mm d}^{-1}$ ) in the southeast United States and decreases (less than  $-0.5 \text{ mm d}^{-1}$ ) along the Texas-Mexico border, where the CMM5 produces less spatially coherent changes of smaller magnitude and of mixed sign. In contrast, the CMM5 projects slightly wetter (drier) conditions in much of the central United States (central-northern Rockies) than the

PCM. More strikingly, the PCM projects temperature increases in the range of 1 to 3°C over most of the United States, with large warming centered in the Midwest and Nevada, whereas the CMM5 simulated warming is generally below 1°C in the eastern United States and approximately 1°C weaker in the southwest United States than the PCM. The above results suggest that the CMM5 downscaling can significantly reduce PCM biases in simulating the present climate and this improvement has important consequences on the future projection of regional climate changes. On the other hand, both the PCM and CMM5 project generally minor changes in summer diurnal cycles (with a few exceptions discussed below) and daily frequency distributions of precipitation and temperature.

[32] For both the present and future climate simulations, the PCM-driven CMM5 results are sensitive to the cumulus parameterization, with strong regional dependence. For example, the Grell scheme produces excellent precipitation diurnal cycles for the central Rockies, central High Plains, central Plains, and LLJ region, whereas the Kain-Fritsch scheme simulates those for the southeast United States and North American Monsoon region in better agreement with observations. Since these CMM5 features are very close to those driven by the R-2 [Liang *et al.*, 2004a] and the driving PCM itself poorly depicts them, the U.S. precipitation diurnal cycle patterns may likely be determined by regional processes and the PCM simulated LBCs are sufficient for reasonable CMM5 downscaling of such patterns. In addition, over the southeast United States, Gulf states, and North American Monsoon region, the PKF produces more frequent intermediate rainfall days than the PGR, generally in better agreement with observations. On the other hand, in the Midwest and Gulf states, the PKF results in too many very warm days, while the PGR simulates more cool days than observed. Thus there is no single cumulus scheme that can capture all key aspects of observations. For the future diurnal cycle changes, the PGR produces a larger temperature amplitude over the central Rockies and North American Monsoon region, both associated with enhanced late afternoon precipitation; and also increased (decreased) rainfall in early morning (evening) over the central Plains and LLJ region, where little change occurs in the temperature cycle. The only noticeable changes by the PKF are identified with precipitation over the central Rockies and central Plains resembling the PGR. It is therefore imperative that ensemble RCM and/or GCM simulations with multiple cumulus schemes are used to more objectively determine the model skill in reproducing observations and better quantify the likely signal and uncertainty in projecting future climate changes. It is also possible that, in a single RCM or GCM run, different cumulus parameterizations (especially those of varying triggering or closure schemes) can be selectively used, individually or in combination, over different regions with distinct climate regimes. We are experimenting with this approach using the ensemble cumulus parameterization of Grell and Dvénényi [2002], where the weights for individual closures can be tuned with regime dependence.

[33] We recognize that the PCM results may not be accurate because the 6-hourly data samples are insufficient for analyses of diurnal cycles, daily means and frequency distributions. However, this by no means changes our

conclusion regarding the PCM failure in reproducing the summer rainfall distributions of the mean and diurnal cycle over the central United States. Such failure is characteristic of the PCM's atmospheric component, the Community Climate Model version 3 (CCM3), and the cumulus parameterization scheme is likely a major contributor as has been consistently documented by other studies [Dai *et al.*, 1999a; Zhang, 2003; Xie *et al.*, 2004; Collier and Zhang, 2005]. We speculate that the deficiency in representing convection is perhaps also the major source for the PCM's large warming in the central United States.

[34] Although we have striven to understand the PCM and CMM5 differences, the exact causes cannot yet be identified. Several hypotheses or mechanisms have been discussed. These mechanisms are, however, not independent, but nonlinearly coupled, and thus very difficult to separately associate with specific model biases. A more difficult obstacle is that many important fields for an objective diagnostic study have not been archived in the PCM simulations; repeating these simulations would be very costly in both human and computational resources. For these reasons, our study and the conclusions drawn are limited. Currently we are using simulations from a new version of the PCM and the HadCM3 under various emission scenarios to drive the CMM5 with both Grell and Kain-Fritsch cumulus schemes. These new modeling results will help determine the likely causes for several key model biases and differences found in this study, and more importantly, quantify the robust signals and uncertainties in projecting future changes in the U.S. regional climate.

[35] **Acknowledgments.** We acknowledge NOAA/FSL and NCSA/UIUC for the supercomputing support. The research was partially supported by the United States Environmental Protection Agency under award EPA RD-83096301-0. The views expressed are those of the authors and do not necessarily reflect those of the sponsoring agencies or the Illinois State Water Survey.

## References

- Bonan, G. (1996), A land surface model (LSM version 1.0) for ecological, hydrological, and atmospheric studies: Technical description and user's guide, *NCAR Tech. Note, NCAR/TN-417+STR*, 150 pp., Natl. Cent. for Atmos. Res., Boulder, Colo.
- Changnon, S. A., J. R. Angel, K. E. Kunkel, and C. M. Lehmann (2004), Climate atlas of Illinois, *ISWS IEM 2004-02*, 309 pp., Ill. State Water Surv., Champaign.
- Chen, F., and J. Dudhia (2001), Coupling an advanced land-surface-hydrology model with the Penn State-NCAR MM5 modeling system. Part I: Model implementation and sensitivity, *Mon. Weather Rev.*, *129*, 569–585.
- Collier, J. C., and G. J. Zhang (2005), Simulation of the North American Monsoon by the NCAR CCM3 and its sensitivity to convection parameterization, *J. Clim.*, in press.
- Dai, A., and K. E. Trenberth (2004), The diurnal cycle and its depiction in the Community Climate System Model, *J. Clim.*, *17*, 930–951.
- Dai, A., F. F. Giorgi, and K. E. Trenberth (1999a), Observed and model-simulated diurnal cycles of precipitation over the contiguous United States, *J. Geophys. Res.*, *104*, 6377–6402.
- Dai, A., K. E. Trenberth, and T. R. Karl (1999b), Effects of clouds, soil moisture, precipitation and water vapor on diurnal temperature range, *J. Clim.*, *12*, 2451–2473.
- Dai, A., G. A. Meehl, W. M. Washington, T. M. L. Wigley, and J. M. Arblaster (2001a), Ensemble simulation of twenty-first century climate changes: Business-as-usual versus CO<sub>2</sub> stabilization, *Bull. Am. Meteorol. Soc.*, *82*, 2377–2388.
- Dai, A., T. M. L. Wigley, B. A. Boville, J. T. Kiehl, and L. E. Buja (2001b), Climates of the twentieth and twenty-first centuries simulated by the NCAR Climate System Model, *J. Clim.*, *14*, 485–519.
- Dai, A., W. M. Washington, G. A. Meehl, T. W. Bettge, and W. G. Strand (2004), The ACPI climate change simulations, *Clim. Change*, *62*, 29–43.

- Davis, C. A., K. W. Manning, R. E. Carbone, S. B. Trier, and J. D. Tuttle (2004), Coherence of warm-season continental rainfall in numerical weather prediction models, *Mon. Weather Rev.*, *131*, 2667–2679.
- Durman, C. F., J. M. Gregory, D. C. Hassell, R. G. Jones, and J. M. Murphy (2001), A comparison of extreme European daily precipitation simulated by a global and a regional climate model for present and future climates, *Q. J. R. Meteorol. Soc.*, *127*, 1005–1015.
- Giorgi, F., L. O. Mearns, C. Shields, and L. McDaniel (1998), Regional nested model simulations of present day and  $2 \times \text{CO}_2$  climate over the central Plains of the U.S., *Clim. Change*, *40*, 457–493.
- Giorgi, F., et al. (2001), Regional climate information: Evaluation and projections, in *Climate Change 2001: The Scientific Basis, Contribution of Working Group I to the Third Assessment Report of the Intergovernmental Panel on Climate Change*, edited by J. T. Houghton et al., pp. 583–638, Cambridge Univ. Press, New York.
- Grell, G. A. (1993), Prognostic evaluation of assumptions used by cumulus parameterizations, *Mon. Weather Rev.*, *121*, 764–787.
- Grell, G. A., and D. Dvňný (2002), A generalized approach to parameterizing convection combining ensemble and data assimilation techniques, *Geophys. Res. Lett.*, *29*(14), 1693, doi:10.1029/2002GL015311.
- Hack, J. J. (1994), Parameterization of moist convection in the NCAR Community Climate Model (CCM2), *J. Geophys. Res.*, *99*, 5551–5568.
- Han, J., and J. O. Roads (2004), U.S. climate sensitivity simulated with the NCEP regional spectral model, *Clim. Change*, *62*, 115–154.
- Higgins, R. W., J. E. Janowiak, and Y.-P. Yao (1996), A gridded hourly precipitation database for the United States (1963–1993), *NCEP/Clim. Predict. Cent. Atlas 1*, 47 pp., U.S. Dep. of Comm., Washington, D. C.
- Kain, J. S., and J. M. Fritsch (1993), Convective parameterization in mesoscale models: The Kain-Fritsch scheme, in *The Representation of Cumulus Convection in Numerical Models, Meteorol. Monogr.*, vol. 46, pp. 165–170, Am. Meteorol. Soc., Boston, Mass.
- Kanamitsu, M., W. Ebisuzaki, J. Woollen, S.-K. Yang, J. J. Hnilo, M. Fiorino, and G. L. Potter (2002), NCEP-DEO AMIP-II Reanalysis (R-2), *Bull. Am. Meteorol. Soc.*, *83*, 1631–1643.
- Kiehl, J. T., J. J. Hack, G. B. Bonan, B. A. Boville, D. L. Williamson, and P. J. Rasch (1998), The National Center for Atmospheric Research Community Climate Model: CCM3, *J. Clim.*, *11*, 1131–1149.
- Kunkel, K. E., K. Andsager, X.-Z. Liang, R. W. Arritt, E. S. Takle, W. J. Gutowski Jr., and Z. Pan (2002), Observations and regional climate model simulations of heavy precipitation events and seasonal anomalies: A comparison, *J. Hydrometeorol.*, *3*, 322–334.
- Leung, L. R., and Y. Qian (2003), The sensitivity of precipitation and snowpack simulations to model resolution via nesting in regions of complex terrain, *J. Hydrometeorol.*, *4*, 1025–1043.
- Leung, L. R., L. O. Mearns, F. Giorgi, and R. L. Wilby (2003), Regional climate research, *Bull. Am. Meteorol. Soc.*, *84*, 89–95.
- Liang, X.-Z., K. E. Kunkel, and A. N. Samel (2001), Development of a regional climate model for U.S. Midwest applications. Part 1: Sensitivity to buffer zone treatment, *J. Clim.*, *14*, 4363–4378.
- Liang, X.-Z., L. Li, A. Dai, and K. E. Kunkel (2004a), Regional climate model simulation of summer precipitation diurnal cycle over the United States, *Geophys. Res. Lett.*, *31*, L24208, doi:10.1029/2004GL021054.
- Liang, X.-Z., L. Li, K. E. Kunkel, M. Ting, and J. X. L. Wang (2004b), Regional climate model simulation of U.S. precipitation during 1982–2002. Part 1: Annual cycle, *J. Clim.*, *17*, 3510–3528.
- Marshall, S., J. O. Roads, and R. J. Oglesby (1997), Effects of resolution and physics on precipitation in the NCAR Community Climate Model, *J. Geophys. Res.*, *102*, 19,529–19,541.
- Mearns, L. O., I. Bogardi, F. Giorgi, I. Matyasovszky, and M. Palecki (1999), Comparison of climate change scenarios generated from regional climate model experiments and statistical downscaling, *J. Geophys. Res.*, *104*, 6603–6621.
- Meehl, G. A., P. R. Gent, J. M. Arblaster, B. Otto-Bliesner, E. C. Brady, and A. P. Craig (2001), Factors that affect amplitude of El Niño in global coupled climate models, *Clim. Dyn.*, *17*, 515–526.
- National Research Council (1991), *Rethinking the Ozone Problem in Urban and Regional Air Pollution*, 500 pp., Natl. Acad. Press, Washington, D. C.
- Pan, Z., J. H. Christensen, R. W. Arritt, W. J. Gutowski Jr., E. S. Takle, and F. Otieno (2001), Evaluation of uncertainties in regional climate change simulations, *J. Geophys. Res.*, *106*, 17,735–17,751.
- Pan, Z., R. W. Arritt, E. S. Takle, W. J. Gutowski Jr., C. J. Anderson, and M. Segal (2004), Altered hydrologic feedback in a warming climate introduces a “warming hole,” *Geophys. Res. Lett.*, *31*, L17109, doi:10.1029/2004GL020528.
- Räisänen, J., U. Hansson, A. Ullerstig, R. Döscher, L. P. Graham, C. Jones, H. E. M. Meier, P. Samuelsson, and U. Willén (2004), European climate in the late twenty-first century: Regional simulations with two driving global models and two forcing scenarios, *Clim. Dyn.*, *22*, 13–31.
- Risbey, J. S., and P. H. Stone (1996), A case study of the adequacy of GCM simulations for input to regional climate change assessments, *J. Clim.*, *9*, 1441–1467.
- Trenberth, K. E., J. C. Berry, and L. E. Buja (1993), Vertical interpolation and truncation of model-coordinate data, *NCAR Tech. Note NCAR/TN-396+STR*, 54 pp., Natl. Cent. for Atmos. Res., Boulder, Colo.
- Vidale, P. L., D. Lüthi, C. Frei, S. I. Seneviratne, and C. Schär (2003), Predictability and uncertainty in a regional climate model, *J. Geophys. Res.*, *108*(D18), 4586, doi:10.1029/2002JD002810.
- Wallace, J. M. (1975), Diurnal variations in precipitation and thunderstorm frequency over the conterminous United States, *Mon. Weather Rev.*, *103*, 406–419.
- Washington, W. M., et al. (2000), Parallel Climate Model (PCM) control and transient simulations, *Clim. Dyn.*, *16*, 755–774.
- Xie, S., M. Zhang, J. S. Boyle, R. T. Cederwall, G. L. Potter, and W. Lin (2004), Impact of a revised convection triggering mechanism on CAM2 model simulations: Results from short-range weather forecasts, *J. Geophys. Res.*, *109*, D14102, doi:10.1029/2004JD004692.
- Zhang, G. J. (2003), Roles of tropospheric and boundary layer forcing in the diurnal cycle of convection in the U.S. Southern Great Plains, *Geophys. Res. Lett.*, *30*(24), 2281, doi:10.1029/2003GL018554.
- Zhang, G. J., and N. A. McFarlane (1995), Sensitivity of climate simulations to the parameterization of cumulus convection in the Canadian Climate Centre general circulation model, *Atmos. Ocean*, *33*, 407–446.
- Zhu, J., and X.-Z. Liang (2005), Regional climate model simulation of U.S. soil temperature and moisture during 1982–2002, *J. Geophys. Res.*, *110*, D24110, doi:10.1029/2005JD006472.

A. Dai, National Center for Atmospheric Research, P. O. Box 3000, Boulder, CO 80307-3000, USA.

K. E. Kunkel, X.-Z. Liang, J. Pan, and J. Zhu, Illinois State Water Survey, University of Illinois at Urbana-Champaign, 2204 Griffith Drive, Champaign, IL 61820-7495, USA. (xliang@uiuc.edu)

J. X. L. Wang, NOAA Air Resources Laboratory, Room 3316, SSMC3, 1315 East West Highway, Silver Spring, MD 20910, USA.